buildings

MDPI

Article

Effects of Size and Flexural Reinforcement Ratio on Ambient-Cured Geopolymer Slag Concrete Beams under Four-Point Bending

Hala Mamdouh [1], Ashraf M. Ali [1], Mostafa A. Osman [1], Ahmed F. Deifalla [2,*] and Nehal M. Ayash [1]

[1] Civil Engineering Department, Faculty of Engineering at Mataria, Helwan University, Cairo 11718, Egypt
[2] Department of Structural Engineering and Construction Management, Faculty of Engineering, Future University in Egypt, New Cairo 11835, Egypt
* Correspondence: ahmed.deifalla@fue.edu.eg

Abstract: With the rise in cement production required by conventional concrete, CO_2 emissions increase, causing pollution to the atmosphere. Geopolymer concrete (GPC) is investigated in the literature as an eco-efficient alternative to conventional concrete (CC). However, most geopolymer studies focus on studying the mechanical properties of GPC, with only limited investigations on the structural performances of structural elements using GPC. The structural behaviors of GPC elements are yet to be completely understood, and there are no current studies on investigating the structural behaviors of geopolymer slag concrete. Thus, this paper investigates the flexural performances of reinforced geopolymer slag concrete beams, focusing on the effects of different beam depths and reinforcement ratios. Five full-scale ambient-cured reinforced geopolymer slag concrete beams were tested under four-point flexure, in addition to one control conventional concrete (CC) beam. The structural performances are evaluated, including the cracking moment, flexural capacity, load–deflection relationship, and crack distribution. The results indicate that the flexural behaviors of GPC beams are comparable to that of the CC beams. Compared to the CC beams, the GPC beams have 7.4% higher flexural moment capacity, 60% lower stiffness, 28% lower ductility, and 18.3% higher toughness. Finally, the Egyptian code of practice ECP 203 and ACI 318 are found to be applicable to safely design under-reinforced GPC flexural beam elements.

Keywords: beam; geopolymer concrete (GPC); slag concrete; conventional concrete (CC); alkali activation; flexural behavior

Citation: Mamdouh, H.; Ali, A.M.; Osman, M.A.; Deifalla, A.F.; Ayash, N.M. Effects of Size and Flexural Reinforcement Ratio on Ambient-Cured Geopolymer Slag Concrete Beams under Four-Point Bending. *Buildings* **2022**, *12*, 1554. https://doi.org/10.3390/buildings12101554

Academic Editors: Binsheng (Ben) Zhang and Wei (David) Dong

Received: 30 June 2022
Accepted: 22 July 2022
Published: 28 September 2022

1. Introduction

Geopolymer concrete (GPC) is a type of concrete made by reacting one or more of alumina–silicate materials with an activator. In most cases, waste materials, such as fly ash or slag from iron and metal products, are used in production of the geopolymer cement which helps lead to a clean environment by reducing carbon dioxide emissions. Hence, the chemical process could reduce the carbon dioxide emission by about 80% more [1] than conventional cement. This concrete is an innovative, eco-friendly material that is used as a replacement for conventional concrete.

The mechanical properties of GPC are investigated in many studies. First, it is well established that the compressive strength of GPC develops more quickly than CC, reaching up to 60 MPa in one day, and it can reach 92.9 MPa after 28 days as reported by Luan et al. [2]. Ashour et al. [3] reported that the geopolymer concrete reached 95% of its final compressive strength in 7 days unlike the conventional concrete, which means that geopolymer concrete can be more efficient in fast-track projects. One of the drawbacks of using GPC is that it requires heat-curing to reach high strengths, but high GPC strengths in ambient curing is possible. Hadi et al. [4] reported a compressive strength of 60.4 MPa after 7 days under air-curing by utilizing pure slag as a main binder. Furthermore, Amer et al. [5] recently

designed a geopolymer pure ground-granulated blast-furnace slag (GGBFS) concrete mix that achieved adequate mechanical properties in addition to a high slump value using ambient curing, making this particular mix sufficiently practical. Other mechanical properties, such as the bond behavior, were investigated in the literature. Fernandez-Jimenez et al. [6] performed pull-out tests and discovered that the GPC bond property is superior to CC. The steel bar broke before slippage from the GPC, while it slipped without breaking from the CC. The maximum pull-out force between GPC and the steel bar was 40% higher than that between CC and the steel bar. Pull-out tests were performed by Zhang et al. [7] on GPC specimens embedded with smooth and ribbed rebars at room temperature and after exposure to 100, 300, 500 and 700 °C. They noticed that GPC exhibits insignificant bond strength reduction up to 300 °C, but suffers significant degradation thereafter. Both at room temperature and after exposure to elevated temperatures, GPC has similar or better bond properties than CC.

Slag, fly ash, silica fume and metakaolin are the most commonly used binder materials in geopolymer concrete [8]. The reaction mechanisms of slag concrete are more complex than the other binders due to the high CaO content. It was found that the presence of Ca has a positive effect on the strength of ambient-cured concrete [9]. Thus, a slag-based geopolymer mix, developed by Amer et al. [5], was chosen for this study.

The flexural behavior is the most important for beams, so it was investigated for GPC beams. Sumajouw et al. [10] studied the structural behavior of fly ash-based geopolymer reinforced concrete beams. They investigated the flexural failure of six under-reinforced concrete beams with various reinforcement ratios. The flexural load-carrying capacity improved as the tensile reinforcement ratio increased. Adak et al. [11] examined the flexural behaviors of nano-silica modified fly ash-based geopolymer reinforced concrete beams and found that the nano silica modified geopolymer concrete exhibits better structural performances than the heat cured geopolymer concrete (without nano silica) and conventional cement concrete samples. Ferdous et al. [12] studied the flexural behaviors of reinforced GPC fly ash-based beams. The maximum load-carrying capacities of the GPC beams were found to be higher than those of the corresponding CC beams in most cases. The GPC and CC beams failed in nearly identical ways, with the same orders of crack diameter, number of cracks, and flexural crack spacing. Du et al. [13] performed bending tests on geopolymer concrete beams and conventional concrete beams, to investigate the effects of concrete strength, rebar ratio and beam depth on the flexural performances. The test results revealed that the flexural behaviors of the GPC beams were comparable to those of the CC beams. When the beam depth increased, the flexural stiffness and load-carrying capacity of the GPC beams were significantly improved. The load-carrying capacity increased significantly as the rebar ratio increased, but the ductility decreased. It was noticed that the flexural performance of GPC beams was unaffected by concrete strength. Moazzenchi and Oskouei [14] examined the bending behavior of the geopolymer concrete beams and reinforced with FRP and steel bars. Four-point flexural tests were carried out on geopolymer concrete and cement concrete beams reinforced with steel, GFRP and CFRP bars. Geopolymer beams reinforced with FRP rebars showed similar results to the reinforced cement beams, and the ductility ratios of the FRP and steel reinforced geopolymer beams are 5% and 34% greater than that of the reinforced OPC concrete, respectively, and these results were comparable to the numerical investigations by Othman et al. [15]. Kumar and Bendapudi [16] investigated the behaviors of geopolymer concrete with various proportions of cement replacement with ground-granulated blast-furnace slag (GGBS) and added metakaolin. Experiments were carried out on the control beams and beams with 100%, 70%, 50% and 30% GGBS and metakaolin, respectively. They found that the load deflection relations of the conventional concrete beams and geopolymer concrete beams are very similar. The cracking moments in the geopolymer beams were lower than those in the conventional concrete beams. Increasing the percentage of metakaolin with respect to GGBS reduces the load-carrying capacity of the beams. Hutagi and Khadiranaikar [17] studied the bending behaviors of Geopolymer Concrete (GPC) beams cured under ambient temperature. Twelve beams were tested under

four-point bending. The percentage of tensile reinforcement and the compressive strength of concrete were taken as the variables while the cross sections of the beams remain constant. The results were found to be similar to those on the conventional cement concrete reinforced beams. Vithiyaluxmi and Senthamilselvi [18] studied the geopolymer RC beams with 30% scrap steel as coarse aggregate and compared with the conventional reinforced cement concrete beams. They found that the performances of the geopolymer beams were marginally better than the conventional beams. The ultimate load-carrying capacity, deflection, service load and ductility factor of the geopolymer beams were higher than those of the conventional RC beams. It is also found that conventional RC theory is suitable to calculate the moment capacity, deflection, and crack width of the geopolymer beams. Ahmed et al. [19] investigated the flexural capacities of GPC (GFRP-RGPC) and ordinary Portland concrete beams reinforced (GFRP-ROPC) with GFRP bars. Nine GFRP-RGPC beams and three GFRP-ROPC beams were tested. The reinforcement ratio and concrete compressive strength types were taken as the variables. Experimental results were compared with the equations provided by ACI 440.1R-15, CSA S806-12, and parabolic stress block method. The results showed the decrease in defection and the increase in the first cracking load by increasing the compressive strength. A slight increase in the defection of the GFRP-RGPC beams and approximately the same value of the ultimate load was observed. The crack widths in the GFRP-RGPC beams are higher than those in the GFRP-ROPC beams. The parabolic stress block method can better predict the flexural capacity rather than the equations in ACI 440.1R-15 and CSA S806-12. Kumaravel et al. [20] studied the flexural behaviors of geopolymer concrete (GPC) beams and control cement concrete beams. The results show that the GPC beams exhibit increases in the flexural strength and deflections at different stages, including service load and peak load stages. Subramanian et al. [21] investigated the flexural behaviors of the geopolymer concrete beams reinforced with basalt (BFRP) and glass (GFRP) fiber reinforced polymer rebars. They found that the basalt and glass reinforced polymer beams demonstrated premature failure and sudden shear failure. The FRP bars helped higher mid-span deflection, crack width and crack propagation, or number and lower cracks spacing than steel bars. Maranan et al. [22] studied the flexural behaviors of geopolymer-concrete beams longitudinally reinforced with a hybrid of GFRP and steel bars. Seven geopolymer-concrete beams with different ratios and configurations of GFRP-to-steel reinforcement were tested. The hybrid beams showed better serviceability and ductility by up to 15% higher than the geopolymer-concrete beams reinforced with GFRP bars only. Increasing the reinforcement ratio increased the overall beam performance. The hybrid beams reinforced with tensile steel reinforcement and compressive GFRP reinforcement obtain higher stiffness and strength at concrete crushing than the beams with hybrid tensile reinforcement. The previous literature indicates that the mix design of geopolymer concrete has a significant effect on the flexural behaviors of GPC beams [23]. However, the mixes investigated in the literature are not practical for use in engineering practice due to the extremely short setting time, or the required heat/steam-curing for GPC to gain adequate mechanical properties, and there is a recommendation to use fibers in geopolymer concrete, as it improves the mechanical characteristics of geopolymer concrete, such as the flexural property [24,25].

Recent advancements in geopolymer mix design produced practical mixes that achieved high compressive strengths and adequate slump values, but their use in structural elements still needs to be investigated. Slag-based geopolymer concrete mixes proved their practicality due to their adequate compressive strength in ambient curing [5]. However, there are currently no studies on investigating the structural behaviors of slag-based geopolymer concrete elements. Thus, this paper provides important results on the flexural behaviors of slag-based geopolymer concrete beams. This study examines the effects of GPC beam depth and reinforcement ratio on the flexural behaviors of reinforced GPC beams. The load–deflection relationship, initial stiffness, post-yield stiffness, ductility, and cracking behavior were examined. Furthermore, the structural behaviors of the GPC beams were

compared to those of the CC beams, and the experimental results were validated according to different design codes.

2. Mix Design

2.1. Raw Materials

2.1.1. Binder

Ordinary portland cement (OPC) for conventional concrete and ground-granulated blast-furnace slag (GGBFS) for geopolymer concrete were used as binders in this study. The used OPC was of grade 42.5 N as per BS-EN 197-1 [26]. Table 1 shows the chemical compositions of the used OPC and GGBFS according to X-ray fluorescence (XRF) analysis.

Table 1. Chemical compositions of GGBFS and OPC by (wt. %).

Component	SiO_2	Al_2O_3	Fe_2O_3	Na_2O	CaO	MgO	K_2O	SO_3	TiO_2	Mn_2O_3
GGBFS	35.41	17.42	1.39	0.49	36.87	6.83	0.97	-	0.11	0.35
OPC	21.07	5.01	3.47	0.29	63.25	2.52	0.19	3.05	-	-

2.1.2. Aggregate

Crushed limestone was used as coarse aggregate, with a nominal maximum size of 9.5 mm, bulk density of 1600 kg/m^3 and specific gravity of 2.66. Natural sand was used as fine aggregate, with nominal maximum size of 4.8 mm, fineness modulus of 2.89, bulk density of 1640 kg/m^3 and specific gravity of 2.55. Figure 1 shows the sieve analyses.

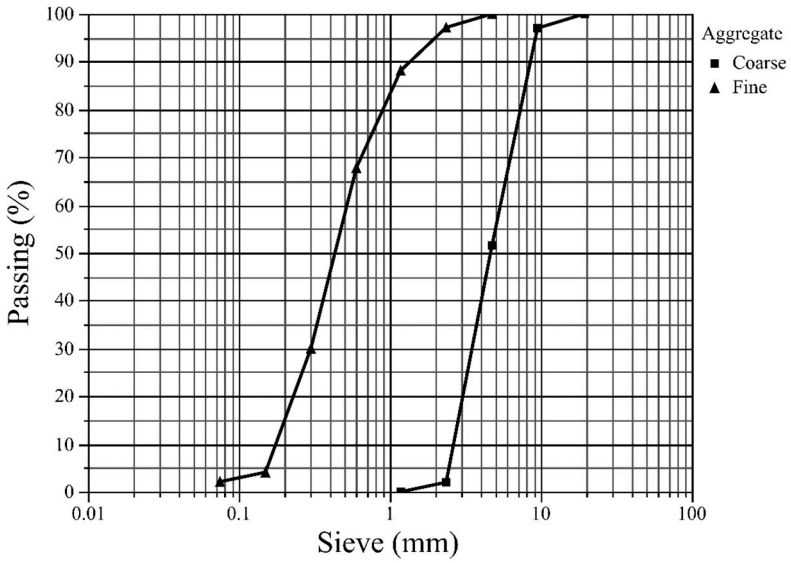

Figure 1. Sieve analyses of the aggregates.

2.1.3. Activator

The activator composed of a mixture of sodium silicate (12% Na_2O, 31% SiO_2 and 57% H_2O) and sodium hydroxide (60.25% Na_2O and 39.75% H_2O) solutions. The sodium hydroxide solution was made by dissolving small solids of sodium hydroxide in potable water, and the sodium silicate solution was obtained from a local producer.

2.2. Mix Proportion

Table 2 shows the mix proportion of slag geopolymer concrete (GPC) and conventional concrete (CC) mixes to produce 1 m^3 of mix.

Table 2. Mix Proportions of the concrete mixes (kg/m^3).

	GGBFS	OPC	C. Agg. *	F. Agg. **	NaOH	Na_2SiO_3	Water	Superplastizer ***
Conventional	-	450	1058	710	-	-	176	12.2
Slag Concrete by Amer et al. [5]	450	-	1093	547	41	131	112	-

Note: * Coarse aggregate, ** Fine aggregate, *** Sikament®—163M.

2.2.1. Conventional Concrete Mix

The mix contained crushed limestone as coarse aggregate, natural sand as fine aggregate and ordinary portland cement, and was mixed with water, having a water–cement ratio of 0.39. Sikament®—163 M was used as superplasticizer admixture for reducing the water to cement ratio without negatively affecting the workability of the mixture.

2.2.2. Geopolymer Concrete Mix

The mix developed by Amer et al. [5] was used here for its adequate compressive strength and ambient curing, which makes its practical use feasible. Figure 2 shows the mixing procedure for the slag geopolymer concrete mix. First, the alkali activator was prepared by dissolving small solids of sodium hydroxide in potable water to make sodium hydroxide solution. Then, it was mixed with the sodium silicate solution. The mixture was left to cool down for three hours since it releases heat. The dry components were mixed for two minutes to ensure homogeneity. Then, the prepared activator solution was slowly poured into the pan mixer while mixing for another two minutes.

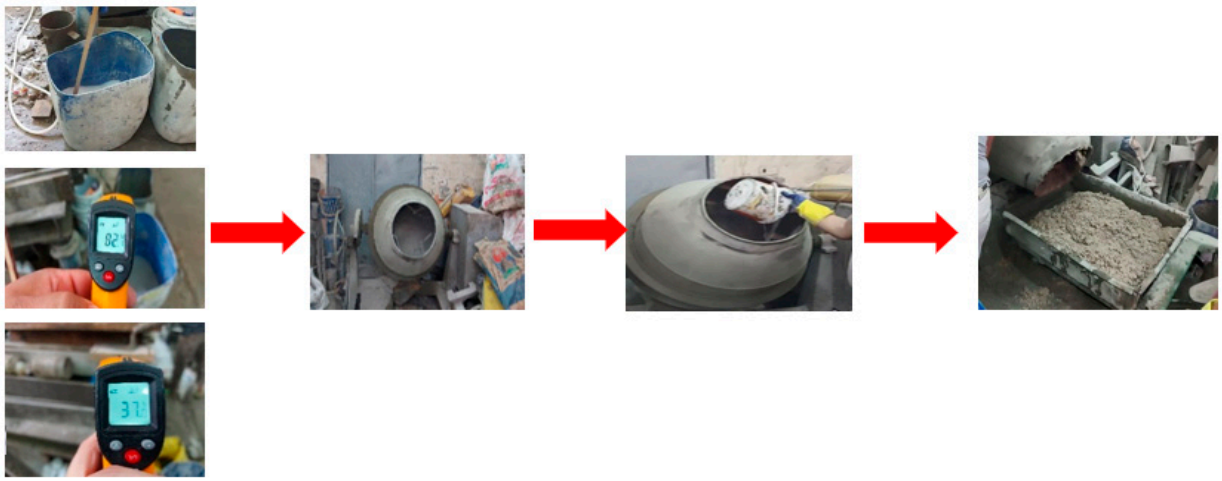

Figure 2. Mixing procedure of the slag geopolymer concrete.

2.3. Mechanical Properties

2.3.1. Concrete

A total of 21 cubic specimens (3 of them were conventional concrete cubes and 18 of them were geopolymer concrete cubes) of 150 mm × 150 mm × 150 mm were prepared to determine the compressive strength (f_{cu}) according to BS EN 12390-1 [27]. Specimens were removed from their molds after 24 h. The GPC specimens were immediately cured in ambient air of temperature 33 ± 2 °C (summer season) until testing, while the CC specimens were first water-cured for 7 days before leaving them in ambient air. Three prismatic specimens of 500 mm × 150 mm × 150 mm were used to determine the modulus of rupture (f_{ctr}) of each mix subjected to a three-point loading test according to ASTM C293 standard [28]. Finally, the moduli of elasticity (E_c) were determined for the CC and GPC mixes using three cylindrical specimens of 150 mm dia. × 300 mm for each mix according to the ASTM C469 standard [29]. The slump tests were performed directly after

mixing according to the ASTM C143 standard [30], and the average value was found to be 215 mm. Despite the high slump values, the used geopolymer mix had a relatively low setting time. Hence, more investigations on increasing the setting time of pure slag mixes are required. Table 3 provides the average mechanical properties of the two mixes after 28 days. The compressive strength of the GPC is higher than that of the CC by approximately 13.8% for the same binder content, but the modulus of rupture and elasticity of the GPC are lower than those of the CC by 24.7% and 27.7%, respectively.

Table 3. The mechanical properties of all mixes after 28 days.

Property	GPC	CC
Compressive strength f_{cu} (MPa)	51.62	45.36
Modulus of rupture f_{ctr} (MPa)	4.38	5.46
Modulus of elasticity E_c (GPa)	25.10	32.30

2.3.2. Reinforcing Steel

High tensile steel bars with diameters of 10, 12 and 16 mm are used. Table 4 provides the mechanical properties of the used reinforcing steel bars of different diameters.

Table 4. Properties of reinforcing steel bars.

	10 mm Diameter (T10)	12 mm Diameter (T12)	16 mm Diameter (T16)
Yield stress (MPa)	542.30	519.60	558.40
Ultimate stress (MPa)	705.10	680.60	779.20
Young's modulus (GPa)	231.20	246.20	248.60

3. Experimental Plan

3.1. Details of the Test Specimens

Five GPC beams and one reference CC beam were tested in total. All beams had the same 2000 mm overall length, an 1800 mm effective span, a 150 mm width, and a 10 mm clear cover. Figure 3 shows the concrete dimensions and the reinforcement of all beam specimens. T10 stirrups with a 100 mm spacing along the beam span were used to avoid shear failure, and all beams were under-reinforced to ensure a ductile failure due to the yielding of steel reinforcement. Two steel bars with a 10 mm diameter (T10) are used as top reinforcement for all tested beams. The beam specimens had various depths and reinforcement ratios. Table 5 provides the test parameters of the tested beams.

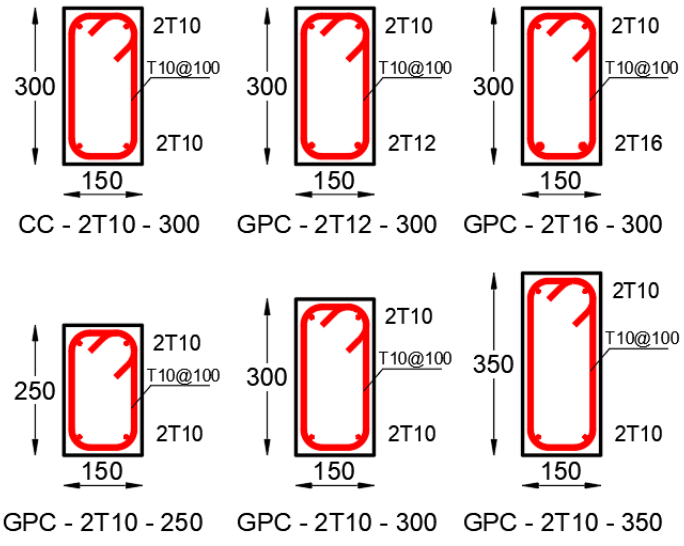

Figure 3. Geometries and reinforcement details of the beams (all dimensions in mm).

Table 5. Beam test parameters.

Beam Label *	Bottom Reinforcement	Reinforcement Ratio, ρ	Total Depth (mm), t
CC-2T10-300	2T10	0.37%	300
GPC-2T10-300	2T10	0.37%	300
GPC-2T12-300	2T12	0.53%	300
GPC-2T16-300	2T16	0.95%	300
GPC-2T10-250	2T10	0.45%	250
GPC-2T10-350	2T10	0.31%	350

* The first part of the beam label indicates the mix type: CC for Conventional Concrete, and GPC for Geopolymer Concrete. The second part of the beam label indicates the number of bars and the diameter of the bottom reinforcement. The last part of the beam label indicates the overall beam depth.

3.2. Test Setup and Procedure

Beams were tested for flexure under four-point symmetric loading test as shown in Figure 4. The spacing between two-point loadings was 600 mm to ensure the pure bending and zero shear region between them as illustrated in Figure 5. A digital load cell was used in the testing procedure. The capacity of the load cell was 5000 kN with a loading rate 1.25 kN per second and was installed at the mid-span of the beam. The beam deflection was measured by three linear variable differential transformers (LVDTs), with one placed at the mid-span and two at the third of span from each side. As shown in Figure 6a,b, two groups of strain gauges were used to monitor the strain components at the specified locations. The first group was the steel reinforcement gauges that were glued on the bottom reinforcing bars at the mid-span of the beam. The second group was the concrete strain gauges, and they were mounted on the top and bottom faces of the mid-span of the beam. The loads, deflections and strains were measured using a data acquisition system. The readings from the load cell and other measurement devices were recorded by a data logger.

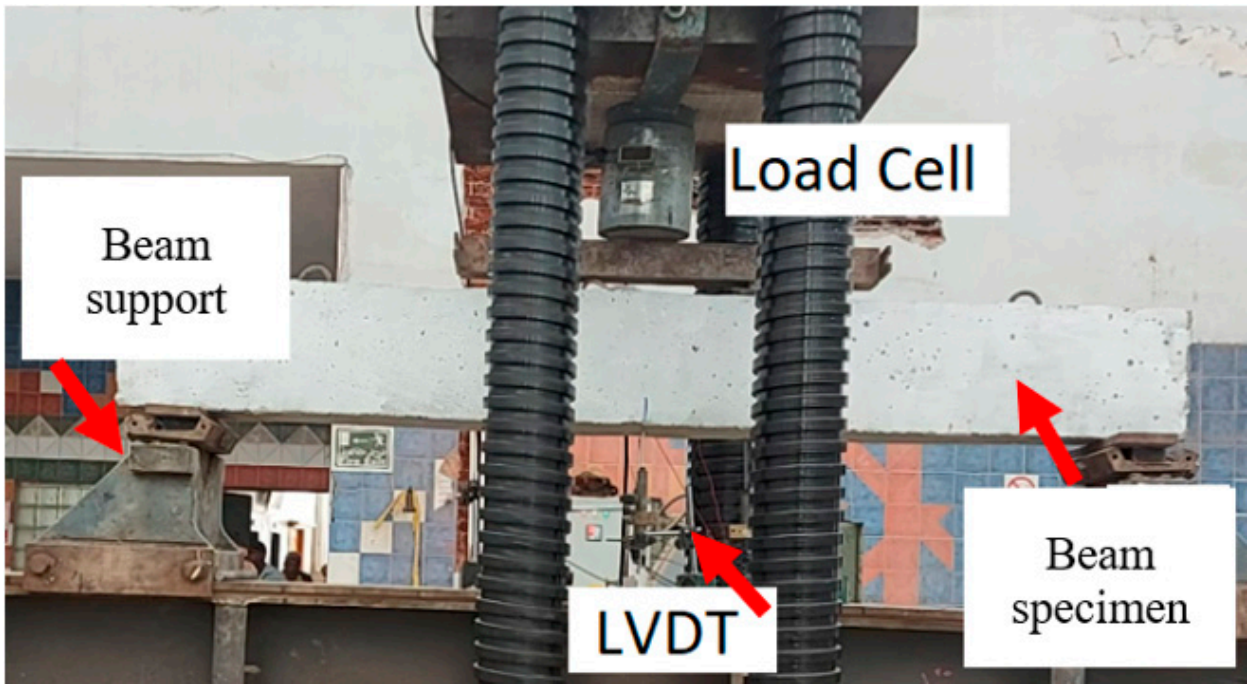

Figure 4. Beam flexure loading test setup and LVDTs locations.

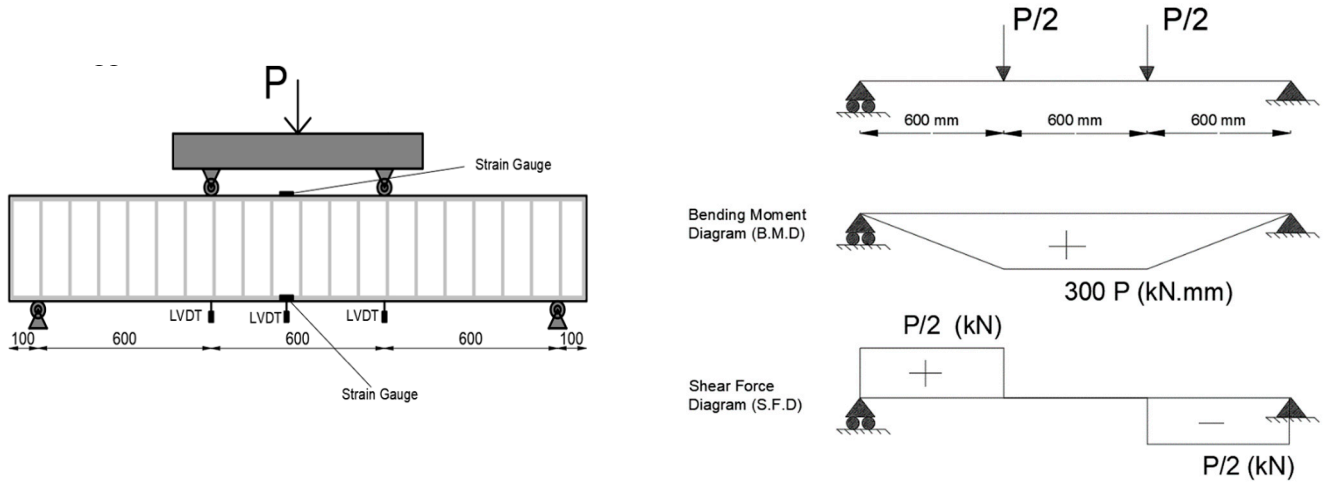

Figure 5. Statically loading system on the beam, with loading, bending moment and shear force.

(**a**) (**b**)

Figure 6. Locations of the strain gauges on (**a**) steel bars and (**b**) concrete.

4. Results and Discussion

4.1. Cracks Distribution

Figure 7 shows the crack distributions for all beam specimens. While increasing the applied load, the widths of the pervious observed cracks increased and new cracks were generated for the cracks initiated in the pure bending zone. When the load exceeded a specific value, diagonal cracks started to develop along the shear span. By comparing Figure 7a,b, the crack patterns in the GPC beams occurred first, with longer cracks and larger crack numbers than those occurring in the CC beams, which supports previous findings [13,31]. Table 6 shows the numbers of shear and flexural cracks in different specimens, in addition to the crack widths. The crack widths are calculated at the service load according to ECP203 [32] as shown in Equation (1). Compared to the CC beams, the equivalent GPC beams have wider crack widths and a larger number of flexural cracks, indicating a better energy dissipation.

Figure 7. Cracks distribution patterns for all tested beams. (**a**) CC—2 T 10—300, (**b**) GPC—2 T 10—300, (**c**) GPC—2 T 12—300, (**d**) GPC—2 T 16—300, (**e**) GPC—2 T 10—250, (**f**) GPC—2 T 10—350.

Table 6. Flexural and shear cracks.

Specimens	Flexural Cracks	Shear Cracks	Crack Width (mm)
CC-2T10-300	5	1	0.23
GPC-2T10-300	7	1	0.26
GPC-2T12-300	9	2	0.24
GPC-2T16-300	12	5	0.22
GPC-2T10-250	6	-	0.27
GPC-2T10-350	9	1	0.21

As the rebar ratio increased, the average spacing of the developed cracks of the GPC beams decreased, and the length and number of cracks increased. The crack initiation was also delayed with the increasing rebar ratio in the GPC beams, since the flexural capacity increased with the increasing rebar ratio. This also resulted in more shear cracks in specimen GPC-2T16-300. Increasing the GPC beam depth increased the average spacing between the developed cracks, the crack length, and the number of cracks. The crack formation was delayed with the increasing beam depth due to the increased capacity. Overall, the failure mechanisms of the GPC beams are similar to those of the CC beams in terms of nominal crack size and distribution, similar to the previous investigations in the literature [12,13,31,33].

$$W_k = \beta \varepsilon_{sm} S_{rm} \quad (1)$$

where:

β is the coefficient relating to average crack width and β = 1.7,
ε_{sm} is the mean steel strain,
S_{rm} is the mean crack spacing in mm.

4.2. Load–Deflection Relationship

Figure 8a,b show the load–deflection curves of the tested beams, with Figure 8a for comparing the tested beams with different rebar ratios and Figure 8b for comparing the tested beams with different depths. The load–deflection curves of the GPC beams are approximately similar to those of the CC beams, as previously found in the literature [12,13,31,33]. The load–deflection curves are divided into three zones: (1) pre-cracking zone, where the load deflection curves linearly increase without any noticeable cracks; (2) pre-yield stage, where cracks start to appear, the crack width increases as the load increases and cracks extend to the top of the beam, which decreases the flexural stiffness; (3) post-yield stage, where more cracks appear and the bottom steel bars yield.

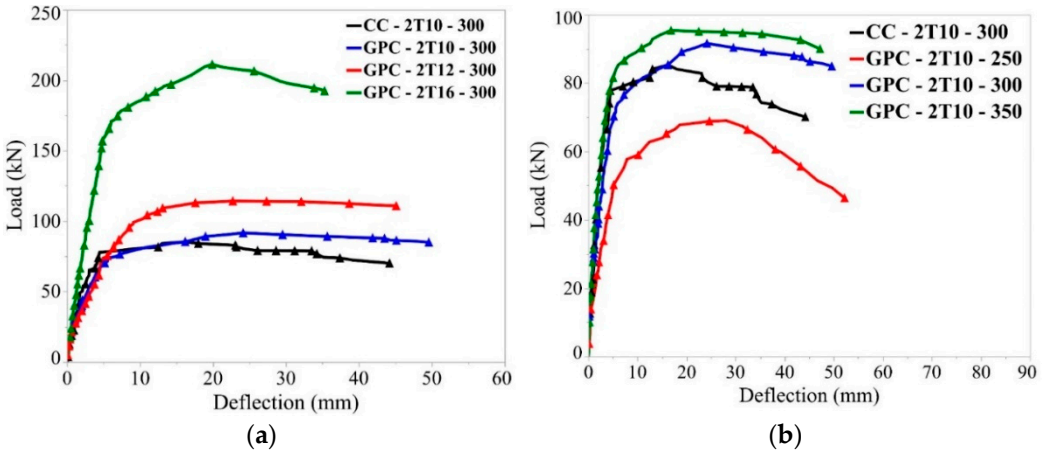

Figure 8. Load–deflection relationship for the tested beams. (**a**) For different reinforcement ratios, (**b**) For different beam depths.

Compared to the CC beam of the same depth and rebar ratio, the GPC beam has 90.3% higher deflection at yielding, and 48.8% higher deflection at failure. It also has 15.2% higher yield load and 7.4% higher failure load. Previous studies on the fly ash-based geopolymer concrete beams indicated that the geopolymer beams had 37–62% higher yield deflections and 20–35% higher failure deflections compared to the CC [31]. The studies [13,31] also showed that the geopolymer beams had 98–154% of the yielding load of the equivalent CC beam, and 100–146% of the failure load of the equivalent CC beam, all depending on the geopolymer concrete mix design.

Table 7 shows the key load and deflection results. For the GPC beams of the same total depth, increasing the reinforcement ratio from 0.37% to 0.95% reduced the deflection at yielding and failure by 9% and 17.4%, respectively, and increased the yielding and failure loads by 224% and 230%, respectively. Previous investigations indicated similar deflection behaviors where increasing the reinforcement ratio decreased the yield and failure deflections [10,13,17,31]. Finally, for the GPC beams with the same reinforcement and variable beam depths, increasing the beam depth from 250 mm to 350 mm reduced the deflections at yielding and failure by 52.6% and 32.5%, and increased the yielding and failure loads by 36.3% and 40.1%.

Table 7. Comparisons of the initial stiffness, post yield stiffness, ductility index and toughness.

Specimens	P_y (kN)	P_u (kN)	Δ_y (mm)	Δ_u (mm)	K_1 (kN/mm)	K_2 (kN/mm)	μ_Δ	Toughness (Joule)
CC-2T10-300	66.5	85.3	3.8	16.2	17.50	1.52	4.26	3368
GPC-2T10-300	76.6	91.6	7.23	24.1	10.59	0.89	3.33	3985
GPC-2T12-300	86.6	114.0	7.08	22.7	12.23	1.75	3.21	4605
GPC-2T16-300	172.0	211.0	6.58	19.9	26.14	2.93	3.02	6320
GPC-2T10-250	58.9	69.02	10.12	28.2	5.83	0.56	2.79	3055
GPC-2T10-350	80.3	96.7	4.8	19.03	16.73	1.15	3.96	4865

4.3. Strains in the Concrete and Steel Bars

Load–strain curves are used mainly to determine the yielding load and yielding deflection, which are used to determine the ductility index and stiffness of the tested beams. Figure 9a,b show the compressive strains of the concrete at the mid-span of the beam specimens. Figure 10 shows the tensile strains of the steel at the mid-span of the beam specimens, with Figure 10a comparing the tested beams with different rebar ratios and Figure 10b comparing the tested beams with different depths. The GPC and CC beams showed similar load–strain trends as there are approximate linear load–strain behaviors

for both steel and concrete until steel yielding. Then, the strains of both steel and concrete rapidly increased until the strain gauges failed. Both the rebar and concrete strains remained unchanged for the increasing depth and reinforcement ratios. However, increasing the rebar ratio increased both rebar and concrete strains at failure, while increasing the beam depth reduced both rebar and concrete strains at failure. These results are similar to previous investigations on geopolymer flexural members [22].

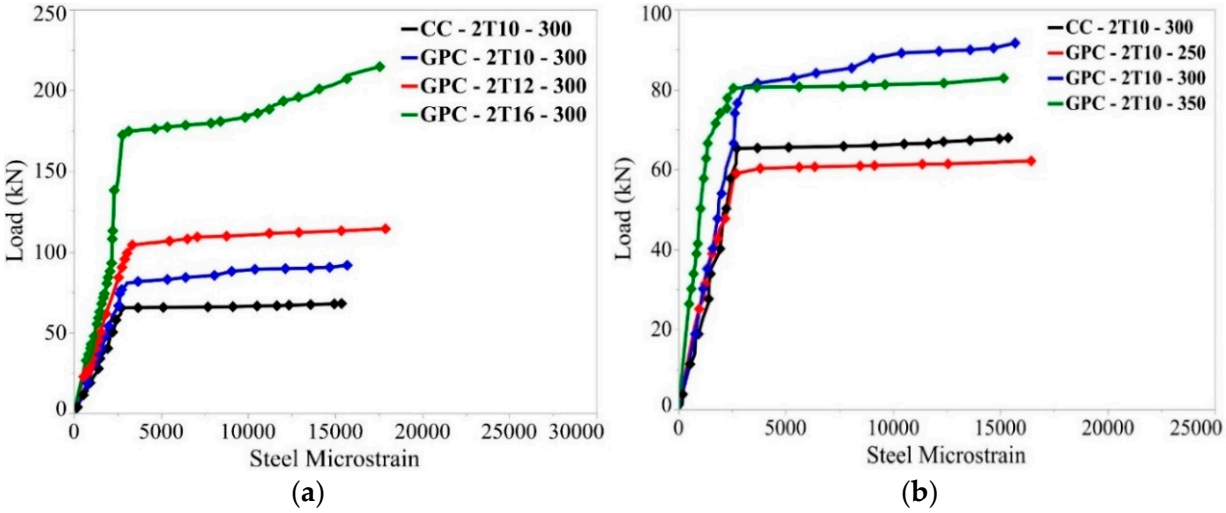

Figure 9. Load–steel rebar strain relationships for the tested beams. (**a**) For different reinforcement ratios, (**b**) For different beam depths.

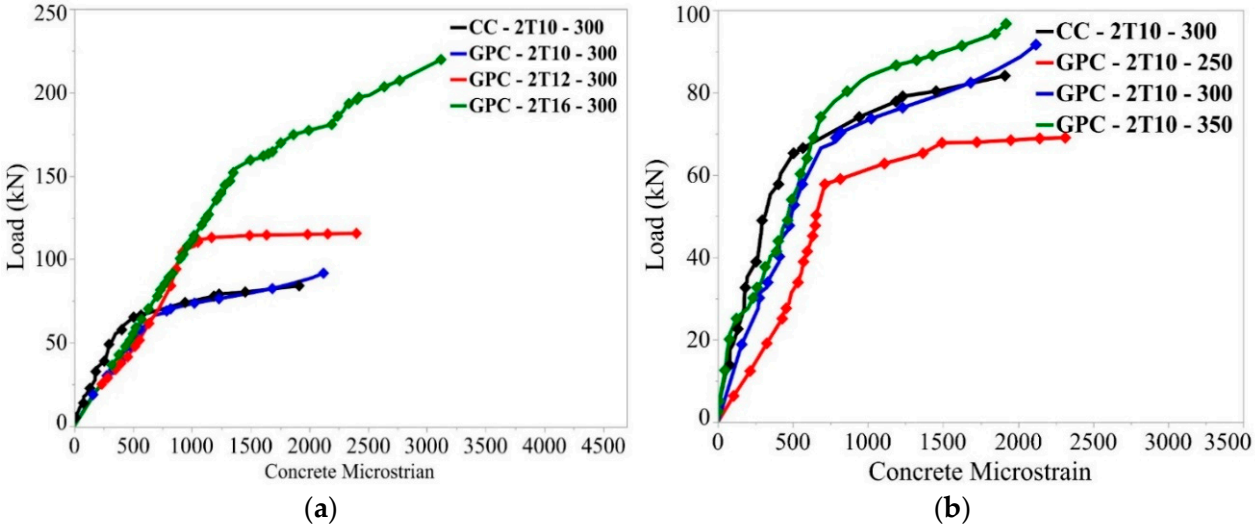

Figure 10. Load–concrete strain relationships for the tested beams. (**a**) Geopolymer beams with different reinforcement ratios, (**b**) Geopolymer beams with different beam depths.

4.4. Stiffness, Ductility and Toughness

The stiffness of the beam can be defined as the slope of the load–deflection curve. The pre-yield stiffness (K_1) and the post-yield stiffness (K_2) are given by Equations (2) and (3). The ductility index (μ_Δ) is also calculated as shown in Equation (4). The ductility of the beam can be defined as the ratio of the deflection at the yield load to the deflection at the ultimate load.

$$K_1 = \frac{P_y}{\Delta_y} \quad (2)$$

$$K_2 = \frac{P_u - P_y}{\Delta_u - \Delta_y} \quad (3)$$

$$\mu_{\Delta} = \frac{\Delta_u}{\Delta_y} \quad (4)$$

where:

K_1 is the pre–yield "initial" stiffness in kN/mm,
P_y is the yielding load in kN,
Δ_y is the deflection at the yielding load in mm,
K_2 is the post–yield "effective" stiffness in kN/mm,
P_u is the ultimate load in kN,
Δ_u is the deflection at the ultimate load in mm.

Table 7 shows the flexural stiffness, ductility and toughness values of the beam specimens. Reductions in the modulus of elasticity and the initial stiffness of the GPC compared to the equivalent CC beams were reported in previous studies [13,33]. For the same depth and reinforcement ratio, the initial and effective stiffness of the GPC beams are lower than those of the CC beams by approximately 60%. The modulus of elasticity of the GPC is also lower than that of the CC by approximately 30%. This is expected since the initial flexural stiffness is affected by the modulus of elasticity. The ultimate loading capacity of the GPC beams is slightly larger than that of the CC beams by 7.4%. Previous investigations found up to 46% load capacity increment [13,31,34]. The deflection of the GPC beams is 48% higher than that of the CC beams, which is similar to the findings by Jeyasehar et al. who observed up to 35% higher deflection in the geopolymer beams compared to the CC beams [31].

The GPC beams showed less ductile behaviors than the CC beams as the ductility values of the GPC beams were 28% lower than that of the equivalent CC beam. Previous investigations found the ductility of fly ash beams to be 92–101% of that in the equivalent CC beam [13]. The toughness (energy absorption) of the beams was determined as the area under the load–deflection curve [35]. For the same depth and reinforcement ratio, the toughness of the GPC beams is found to be higher than the equivalent CC beam by up to approximately 18.3%, indicating a better energy dissipation. This is also supported by the wider crack distributions in the GPC beams.

Figures 11–13 show the values of the initial and effective stiffnesses, ductility index and toughness for the Geopolymer tested beams, with Figures 11a, 12a and 13a for different rebar ratios and Figures 11b, 12b and 13b for different beam depths. When the rebar ratio increased from 0.37% to 0.95%, the cracking moment increased by 24%, the initial stiffness increased by 147%, the effective stiffness increased by 229%, and the toughness increased by 58.6%. The ductility index decreased by 10.2% with the increasing rebar ratio. Having a higher rebar ratio corresponds to a higher energy dissipation, which is evident in the wider crack distribution shown in Figure 7d for beam specimen GPC-2T16-300. This led to tougher, more brittle behavior for the GPC beam with a higher rebar ratio.

When the beam depth increased from 250 mm to 350 mm, the initial stiffness increased by 181%, the effective stiffness increased by 105%, the toughness increased by 59%, and the ductility index increased by 42%. Increasing the beam depth increased the section inertia, which increased the stiffness. Additionally, for the same reinforcement (2T10), increasing the beam depth reduced the rebar ratio (from 0.45% to 0.31%). This reduction in the reinforcement ratio led to less tough, more ductile behavior. Similar relations between the rebar ratio and the ductile behavior of GPC beams have also been asserted in previous research [13].

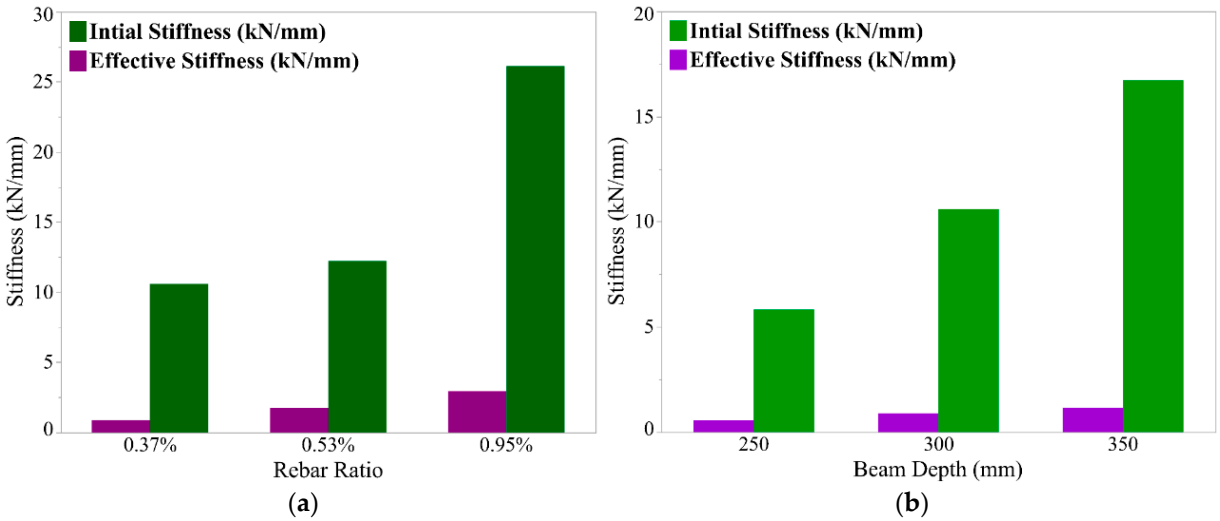

Figure 11. Initial and effective stiffnesses for the geopolymer tested beams. (**a**) For different rebar ratios, (**b**) For different beam depths.

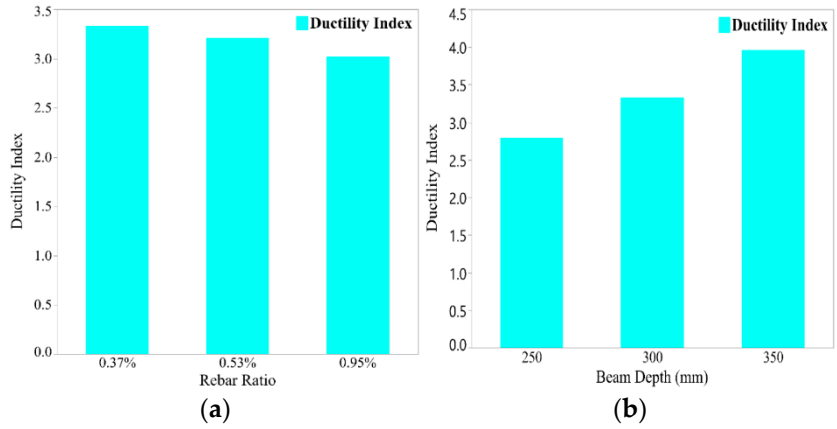

Figure 12. Ductility indexes for the geopolymer tested beams. (**a**) For different rebar ratios, (**b**) For different beam depths.

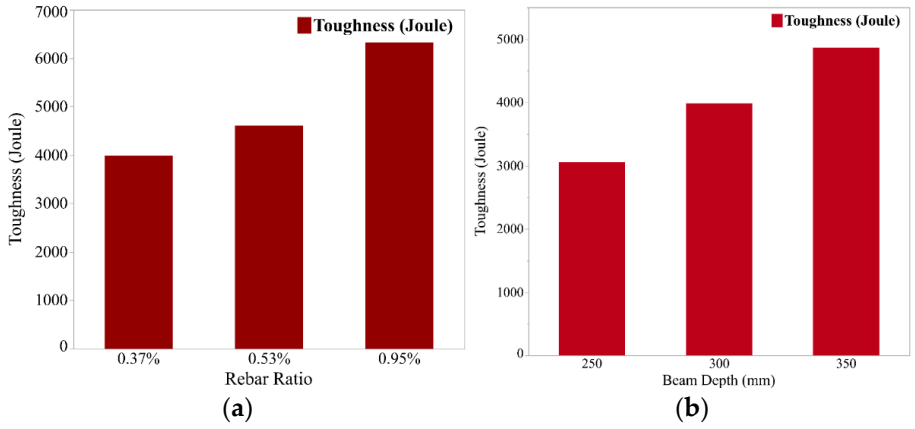

Figure 13. Toughness of the geopolymer tested beams. (**a**) For different rebar ratios, (**b**) For different beam depths.

4.5. Cracking and Ultimate Moments

Table 8 shows the experimental and predicted cracking moments. The predicted cracking moment is calculated with Equation (5). The experimental cracking moment is smaller by an average of 10% for all beams. The experimental cracking moments are reduced because of the additional stresses resulting from shrinkage and the presence of hair cracks due to temperature effects. For the same beam depth and reinforcement ratio, the experimental cracking moment of the GPC beams was less than that of the CC beams, since the modulus of rupture of the GPC is found to be lower than the modulus of rupture of the CC.

$$M_{cr} = \frac{f_{ctr}\ I_g}{y_t} \tag{5}$$

where:

M_{cr} is the theoretical cracking moment in kNm,
f_{ctr} is the modulus of rupture of concrete in kN/m^2,
I_g is the gross moment of inertia of beam section in m^4,
y_t is the distance from the tension side of beam to the neutral axis in m.

Table 8. Experimental and theoretical cracking and ultimate moments of the tested beams.

Specimens	*Mcr* (kNm)			*Mu* (kNm) by ECP203			*Mn* (kNm) by ACI318	
	Mexp	*Mtheo*	*Mexp/Mtheo*	*Mexp*	*Mtheo*	*Mexp/Mtheo*	*Mtheo*	*Mexp/Mtheo*
CC-2T10-300	12.0	14.2	0.85	25.59	23.47	1.09	23.48	1.09
GPC-2T10-300	9.9	11.4	0.87	27.48	23.56	1.17	23.58	1.17
GPC-2T12-300	10.8	11.8	0.92	34.2	32.01	1.07	32.16	1.06
GPC-2T16-300	12.3	12.9	0.95	63.3	58.42	1.08	59.19	1.07
GPC-2T10-250	7.5	8.0	0.93	20.7	19.31	1.07	19.32	1.07
GPC-2T10-350	12.6	15.2	0.83	29.01	27.82	1.04	27.83	1.04

Notes: M_{cr}—cracking moment, M_u—ultimate moment, M_n—nominal moment, M_{exp}—experimental results, M_{theo}—predicted results.

The predicted ultimate moment is calculated with Equation (6) according to ECP203 [32] and calculated with Equation (7) according to ACI318 [36]. For the beams with the same depth and reinforcement ratio, the ultimate moment of the GPC beam was 7.4% higher than that of the CC beam. Furthermore, the experimental-to-predicted ultimate moment ratio for the GPC beams ranged between 1.04 and 1.17 with an average of 1.09, compared to 1.09 for the CC beam. This indicates that the design codes ECP203 and ACI 318 could be used to design flexural GPC beams. Previous investigations used other building codes to validate the tested geopolymer concrete beams. The test to prediction moment ratios of the GPC beams were found to be 0.98–1.28 as per AS3600 [10] and 0.95–1.10 as per GB50010 [13].

$$a = \frac{f_y\ A_s}{\frac{2}{3}\ f_{cu}\ b} \tag{6}$$

$$M_u = f_y\ A_s \left(d - \frac{a}{2}\right) \tag{7}$$

where:

M_u is the theoretical ultimate moment in kNm,
f_y is the steel yielding stress in MPa,
A_s is the main steel area in mm^2,
d is the effective depth of beam in mm,
a is the concrete compression zone depth in mm,
b is the beam width in mm.

$$\beta_1 = 0.85 - \frac{0.05\,(f'_c - 28)}{7} \geq 0.65; \text{for } 28 \text{ MPa} < f'_c < 55 \text{ MPa} \quad (8)$$

$$c = \frac{f_y\, A_s}{0.85 f'_c\, \beta_1\, b}; \quad (9)$$

$$M_n = f_y\, A_s \left(d - \frac{\beta_1\, c}{2}\right) \quad (10)$$

where:

M_n is the unfactored theoretical nominal moment in kNm,
f'_c is the cylinder compressive strength of concrete in MPa,
β_1 is the ratio of the depth of the equivalent stress block to the actual neutral axis depth.

Generally, increasing the rebar ratio led to the improvements in the moment capacity, effective stiffness and toughness, but did not improve the ductility. On the other hand, increasing the beam depth with constant reinforcements led to the improvement in the ductility in addition to the moment capacity, effective stiffness and toughness. Figure 14 shows the cracking and ultimate moments for the tested GPC beams, with Figure 14a for different rebar ratios and Figure 14b for different beam depths. When the rebar ratio increased from 0.37% to 0.95%, the cracking moment increased by 24%, and the ultimate moment increased by 130%. Previous investigations also reported 56–71% increases in the cracking moment for increasing the reinforcement ratio from 0.66% to 2.71%, depending on the mix strength [13]. Additionally, when the beam depth increased from 250 mm to 350 mm, the cracking moment increased by 68% and the ultimate moment increased by 40%.

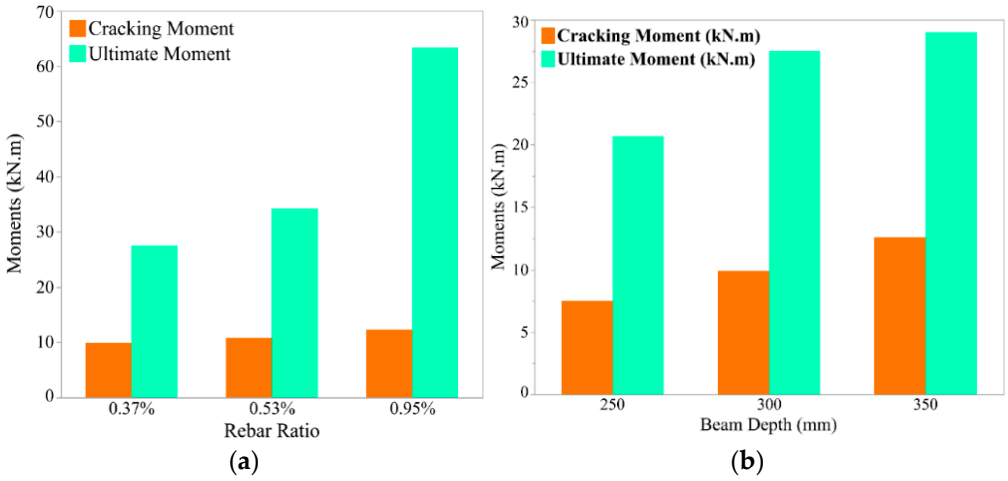

Figure 14. Cracking and ultimate moments for the geopolymer tested beams. (**a**) For different rebar ratios, (**b**) For different beam depths.

5. Conclusions

This study investigates the effects of the beam depth and rebar ratio on the flexural behaviors of the ambient-cured slag geopolymer concrete beams. The results presented in this research are limited to the dimensions, reinforcements and loading conditions studied. The main conclusions derived from the results can be summarized as follows:

1. The load-carrying capacity of the GPC beams increased with increasing both the beam depth and rebar ratio. Compared to the CC beams, the flexural moment capacity of the reinforced GPC beams was 7.4% higher, and the cracking moment was 17.5% lower due to the lower modulus of rupture.
2. The initial and effective stiffnesses of the GPC beams increased with increasing both the beam depth and rebar ratio. Compared to the CC beams, the initial and effective

stiffnesses of the GPC beams were lower by 60%. Furthermore, the deflection of the GPC beams was 48.7% higher due to their lower modulus of elasticity.

3. Increasing the beam depth significantly increases the beam ductility but using a higher rebar ratio decreases the beam ductility. However, the toughness of the GPC beams increased by increasing either beam depth or rebar ratio. Compared to the CC beams, the ductility of GPC beams was 28% lower, and the toughness was 18.3% higher.
4. The crack distributions of the GPC beams occurred earlier, in more numbers and longer than those appearing in the CC beams. As the rebar ratio increased, the appearance of the cracks was retarded, and the average spacing of the developed cracks on the GPC beams decreased and the number of cracks increased. Increasing the GPC beam depth led to the delay in the occurrence of the cracks and the increase in the average spacing of the developed cracks.
5. The Egyptian code of practice ECP203 and ACI318 should be applicable in predicting the flexural moment capacity of under-reinforced GPC beams.

6. Future Recommendations

Though this study presents important results on the flexural behaviors of the slag-based geopolymer concrete beams, the literature is still lacking. More studies on the effects of different mix designs on the structural behaviors of geopolymer concrete elements. Beside the flexural behaviors, the shear behaviors of geopolymer concrete members should also be investigated. Finally, the behaviors of other geopolymer concrete structural members, e.g., slabs, columns, etc., should be studied.

Author Contributions: Conceptualization, A.F.D. and H.M.; methodology, A.M.A. and M.A.O.; software, N.M.A.; validation, A.F.D. and H.M.; formal analysis, A.M.A. and M.A.O.; investigation, A.M.A. and M.A.O.; resources, N.M.A.; data curation, A.M.A. and M.A.O.; writing—original draft preparation, A.F.D. and H.M.; writing—review and editing, M.A.O. and N.M.A.; visualization, N.M.A.; supervision, A.F.D. and H.M.; project administration, A.F.D. and H.M.; funding acquisition, A.F.D. All authors have read and agreed to the published version of the manuscript.

Funding: This research received no external funding.

Institutional Review Board Statement: Not applicable.

Informed Consent Statement: Not applicable.

Data Availability Statement: All data related to the study was reported within the study.

Conflicts of Interest: The authors state that they have no known competing financial interests or personal ties that would appear to have influenced the work presented in this study.

References

1. Van Deventer, J.S.J.; Provis, J.L.; Duxson, P. Technical and commercial progress in the adoption of geopolymer cement. *Miner. Eng.* **2012**, *29*, 89–104. [CrossRef]
2. Luan, C.; Shi, X.; Zhang, K.; Utashev, N.; Yang, F.; Dai, J.; Wang, Q. A mix design method of fly ash geopolymer concrete based on factors analysis. *Constr. Build. Mater.* **2021**, *272*, 121612. [CrossRef]
3. Ashour, A.Z.; Gallab, A.H.; Khafaga, M.A.; Rashad, A.; Kohail, M. Using metakaolin and ground granulated blast furnace slag in production of geopolimer concrete. *J. Tianjin Univ. Sci. Technol.* **2021**, *54*, 84–112. [CrossRef]
4. Hadi, M.N.S.; Farhan, N.A.; Sheikh, M.N. Design of geopolymer concrete with GGBFS at ambient curing condition using Taguchi method. *Constr. Build. Mater.* **2017**, *140*, 424–431. [CrossRef]
5. Amer, I.; Kohail, M.; El-Feky, M.S.; Rashad, A.; Khalaf, M.A. Characterization of alkali-activated hybrid slag/cement concrete. *Ain Shams Eng. J.* **2021**, *12*, 135–144. [CrossRef]
6. Fernandez-Jimenez, A.M.; Palomo, A.; Lopez-Hombrados, C. Engineering properties of alkali-activated fly ash concrete. *Mater. J.* **2006**, *103*, 106–112. [CrossRef]
7. Zhang, H.Y.; Kodur, V.; Wu, B.; Yan, J.; Yuan, Z.S. Effect of temperature on bond characteristics of geopolymer concrete. *Constr. Build. Mater.* **2018**, *163*, 277–285. [CrossRef]
8. Amer, I.; Kohail, M.; El-Feky, M.S.; Rashad, A.; Khalaf, M.A. A review on alkali-activated slag concrete. *Ain Shams Eng. J.* **2021**, *12*, 1475–1499. [CrossRef]

9. Aziz, I.H.; Abdullah, M.M.A.B.; Mohd Salleh, M.A.A.; Azimi, E.A.; Chaiprapa, J.; Sandu, A.V. Strength development of solely ground granulated blast furnace slag geopolymers. *Constr. Build. Mater.* **2020**, *250*, 118720. [CrossRef]
10. Sumajouw, D.; Hardjito, D.; Wallah, S.E.; Rangan, B.V. Behaviour and strength of reinforced fly ash-based geopolymer concrete beams. *Civ. Eng. Dimens.* **2005**, *6*, 1020.
11. Adak, D.; Sarkar, M.; Mandal, S. Structural performance of nano-silica modified fly-ash based geopolymer concrete. *Constr. Build. Mater.* **2017**, *135*, 430–439. [CrossRef]
12. Ferdous, W.; Manalo, A.; Khennane, A.; Kayali, O. Geopolymer concrete-filled pultruded composite beams—Concrete mix design and application. *Cem. Concr. Compos.* **2015**, *58*, 1–13. [CrossRef]
13. Du, Y.; Wang, J.; Shi, C.; Hwang, H.J.; Li, N. Flexural behavior of alkali-activated slag-based concrete beams. *Eng. Struct.* **2021**, *229*, 111644. [CrossRef]
14. Moazzenchi, S.; Oskouei, A.V. A comparative experimental study on the flexural behavior of geopolymer concrete beams reinforced with FRP bars. *J. Rehabil. Civ. Eng.* **2023**, *11*, 21–42. [CrossRef]
15. Zinkaah, O.H.; Alridha, Z.; Alhawat, M. Numerical and theoretical analysis of FRP reinforced geopolymer concrete beams. *Case Stud. Constr. Mater.* **2022**, *16*, e01052. [CrossRef]
16. Kumar, P.U.; Bendapudi, S. Flexural behaviour of reinforced Geopolymer concrete beams with GGBS and metakaoline. *Int. J. Civ. Eng. Technol.* **2016**, *7*, 260–277.
17. Hutagi, A.; Khadiranaikar, R.B. Flexural behavior of reinforced geopolymer concrete beams. *Int. Conf. Electr. Electron. Optim. Tech. ICEEOT* **2016**, *2016*, 3463–3467. [CrossRef]
18. Vithiyaluxmi, V.B.; Senthamilselvi, P. Flexural behaviour of geopolymer reinforced concrete beam with partial replacement of coarse aggregate by using steel slag. *Int. Res. J. Eng. Technol.* **2021**, *8*.
19. Ahmed, H.Q.; Jaf, D.K.; Yaseen, S.A. Flexural capacity and behaviour of geopolymer concrete beams reinforced with glass fibre-reinforced polymer bars. *Int. J. Concr. Struct. Mater.* **2020**, *14*, 1–16. [CrossRef]
20. Kumaravel, D.; Thirugnanasambandam, S. Flexural behaviour of geopolymer concrete beams. *Int. J. Adv. Eng. Res. Stud.* **2013**, *3*, 2249–8974.
21. Subramanian, N.; Solaiyan, E.; Sendrayaperumal, A.; Lakshmaiya, N. Flexural behaviour of geopolymer concrete beams reinforced with BFRP and GFRP polymer composites. *Adv. Struct. Eng.* **2022**, *25*, 954–965. [CrossRef]
22. Maranan, G.B.; Manalo, A.C.; Benmokrane, B.; Karunasena, W.; Mendis, P.; Nguyen, T.Q. Flexural behavior of geopolymer-concrete beams longitudinally reinforced with GFRP and steel hybrid reinforcements. *Eng. Struct.* **2019**, *182*, 141–152. [CrossRef]
23. Mo, K.H.; Alengaram, U.J.; Jumaat, M.Z. Structural performance of reinforced geopolymer concrete members: A review. *Constr. Build. Mater.* **2016**, *120*, 251–264. [CrossRef]
24. De Azevedo, A.R.G.; Cruz, A.S.A.; Marvila, M.T.; De Oliveira, L.B.; Monteiro, S.N.; Vieira, C.M.F.; Fediuk, R.; Timokhin, R.; Vatin, N.; Daironas, M. Natural fibers as an alternative to synthetic fibers in reinforcement of geopolymer matrices: A comparative review. *Polymers* **2021**, *13*, 2493. [CrossRef]
25. Yanou, R.N.; Kaze, R.C.; Adesina, A.; Nemaleu, J.G.D.; Jiofack, S.B.K.; Djobo, J.N.Y. Performance of laterite-based geopolymers reinforced with sugarcane bagasse fibers, Case stud. *Constr. Mater.* **2021**, *15*, e00762. [CrossRef]
26. *BS EN 197-1*; Cement—Part 1 Composition, Specifications and Conformity Criteria for Common Cements; British Standards Institution (BSI): London, UK, 2011.
27. *BS EN 12390-1*; Concrete—Part 1: Shape Dimensions and Other Requirements for Specimens and Moulds; British Standards Institution (BSI): London, UK, 2011.
28. *ASTM C293*; Flexural Strength of Concrete (Using Simple Beam with Center-Point Loading; American Society for Testing and Materials (ASTM): West Conshohocken, PA, USA, 2002.
29. *ASTM C469/C469M-14*; Standard Test Method for Static Modulus of Elasticity and Poisson's Ratio of Concrete in Compression; American Society for Testing and Materials (ASTM) International: West Conshohocken, PA, USA, 2014.
30. *ASTM C143/C143M*; Standard Test Method for Slump of Hydraulic Cement Concrete; American Society for Testing and Materials (ASTM): West Conshohocken, PA, USA, 2015; pp. 1–4.
31. Antony, J.C.; Saravanan, G.; Salahuddin, M.; Thirugnanasambandam, S. Development of fly ash based geopolymer precast concrete elements. *Asian J. Civ. Eng.* **2013**, *14*, 605–615.
32. ECP Committee. *ECP 203 Egyptian Code for Design and Construction of Concrete Structures (ECP 203-2020)*, 5th ed.; Housing and Building National Research Center: Cairo, Egypt, 2020.
33. Ren, J.; Chen, H.; Sun, T.; Song, H.; Wang, M. Flexural behaviour of combined FA/GGBFS geopolymer concrete beams after exposure to elevated temperatures. *Adv. Mater. Sci. Eng.* **2017**. [CrossRef]
34. Yost, J.R.; Radlińska, A.; Ernst, S.; Salera, M.; Martignetti, N.J. Structural behavior of alkali activated fly ash concrete. Part.Structural testing and experimental findings. *Mater. Struct. Constr.* **2013**, *46*, 449–462. [CrossRef]
35. Köksal, F.; Rao, K.S.; Babayev, Z.; Kaya, M. Effect of steel fibres on flexural toughness of concrete and RC beams. *Arab. J. Sci. Eng.* **2022**, *47*, 4375–4384. [CrossRef]
36. *ACI 318*; Building Code Requirements for Structural Concrete (ACI 318-19) and Commentary (ACI 318R-19); The American Concrete Institute (ACI): Farmington Hills, MI, USA, 2019.